UNIVERSITY OF ALBERTA

DEPARTMENT OF MINERAL ENGINEERING

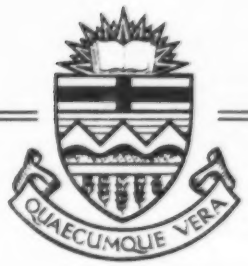

CONTRACT SERIAL NO: OSV84-00026
CONTRACTOR: University of Alberta
REQUISITION NO: 23440-0-9197-1

Welding Engineering Report No.8

EMR Contract DSS 05SU.23440-0-9197

NARROW GAP WELDING OF CR-MO STEELS

by

A.C. Bicknell

and

B.M. Patchett

"This report was prepared as an account of work sponsored by a Department of the Federal Government of Canada. Neither the Federal Government of Canada nor any agency thereof, nor any contractor or subcontractor, nor any of their employees, makes any warranty, expressed or implied, or assumes any legal liability or responsibility for any third parties use of or the results of such use of any information, apparatus, product or process disclosed in this report, or represents that its use by such third party would not infringe privately owned rights".

49 pp

MICROMEDIA

ABSTRACT

G.M.A.W. narrow gap welds, ASME qualified and experimental, were made to study the effects of shielding gas oxidation potential on the metallurgical and mechanical properties of 2.25% Cr - 1% Mo weld metal. Shielding gas compositions ranged from medium oxidation, Ar-20%CO_2, to a reducing mixture of Ar-2%CO_2-0.5%H_2. The investigation showed that there was a correlation between the oxidation potential of the shielding gas and the following: residual weld metal oxygen; oxygen related inclusions; weld metal chemical analysis; and weld metal microstructures. Results show that the chemistry of the electrodes designed for high and medium oxidation use will have to be altered to suit the lower potential gases, increased weld metal deoxidant levels decreased the impact resistance of the steel in spite of favourable reductions in weld metal oxygen and inclusion content.

A new experimental rotating arc welding torch has been designed. The design is adapted from principles developed by NKK. The torch was constructed at the University of Alberta and is for in-house experiments only. It will allow the testing of flux-cored and powder-cored wires of various diameters to be fully tested, which is not possible with the present NKK machine, due to the power source design, which limits procedures to solid wires of two specific diameters, namely 1.2 and 1.6 mm. The new torch will be used with a Hobart 650 ampere power source to falcilitate operation at higher currents than are possible with the standard NKK torch.

TABLE OF CONTENTS

INTRODUCTION	Page 1
EXPERIMENTAL PROGRAM	Page 2
RESULTS	Page 5
Weld Metal Residual Elements	Page 6
Weld Metal Chemistries	Page 7
Inclusion Contents	Page 8
Mechanical Properties	Page 9
Microstructures	Page 10
DISCUSSION	Page 11
CONCLUSIONS	Page 13
REFERENCES	Page 14
TABLES	Page 15
FIGURES	Page 21
APPENDIX A	Page 33
APPENDIX B	Page 36
APPENDIX C	Page 43

INTRODUCTION

Gas metal arc welding of steels relies heavily on oxygen additions to an inert shielding gas to produce several desirable results. Compared to an inert gas, the inert-oxidizing combinations, mostly argon plus 2-5% oxygen or argon and/or helium plus 10-35% carbon dioxide, produce higher electron emission in the cold cathode materials resulting in greater arc stability. The temperature and velocity of the arc plasma also increase in an oxidizing atmosphere via the dissociation of the higher ionization potential polyatomic gases. The temperature increase produces deeper and more uniform penetration (1) of the weld bead by eliminating the "finger" penetration of inert gases, while the velocity of the plasma augments the transfer of the molten droplets from the electrode resulting in more regular metal transfer intervals.

Microstructures of the weld metal are also affected by the oxidation effect of the shielding, residual weld metal oxygen imparted by the shielding has both beneficial and detrimental effects. Optimum levels of weld metal oxygen promote the formation of acicular ferrite in the solidifying weld pool. Excessive levels of weld metal oxygen increase the number and volume of oxide inclusions in the weld, which decrease the upper shelf charpy impact strength of the steel by supplying an increased number of sites for microvoid coalescence, lowering the steels ability to resist ductile tearing.

Narrow gap welding of Cr-Mo steels with the Twist-wire GMAW process developed by KOBE Steel of Japan, generally uses a

shielding gas mixture of argon plus 15-20% CO_2. These gases are used in combination with special electrodes chemically formulated to produce welds with the desired chemistries and microstructures which meet the low temperature requirements for the given grade and class of steel being welded. It has been shown in the CANMET research project (2,3) that while the KOBE Twistwire process, using a shielding gas mixture of 80%Ar-20%CO_2, produced a weld with suitable low temperature charpy values because of its unique microstructures, the properties at room temperature did not show as dramatic an improvement as comparable submerged arc welds with lower weld metal oxygen and inclusion contents, Fig. 1. It was noted that there was a correlation between the room temperature charpy values of the welds and the inclusion content: residual oxygen; and sulfur levels.

This report will deal with the experimental procedures, and results, that were conducted to evaluate the metallurgical effects of several lower oxidizing potential shielding gases on the weld metal properties of the KOBE Twistwire electrode for 2.25Cr-1Mo pressure vessel steels. Further procedural effects will be assessed with a new rotating arc torch built for in-house experiments with flux and powder-cored wires supplied by CONARCO.

EXPERIMENTAL PROGRAM

A total of eight welds, all using the same reel of twistwire electrode, were made for comparison to the first weld made for the original CANMET contract, parameters of the welds are given in Table 1, and the following numerical designations were used to identify the welds.

WELD #	SHIELDING GAS	BASE METAL
1	Ar-20%CO_2	38mm SA387 Gr.22 Cl.2
2	Ar-2%CO_2-0.5%H_2	38mm SA387 Gr.22 Cl.2
3	Ar-2%CO_2-0.5%H_2	50mm SA387 Gr.22 Cl.2
4	Ar-2%CO_2-0.5%H_2	63mm SA387 Gr.11 Cl.1
5	Ar-2%CO_2	63mm SA387 Gr.11 Cl.1
6	Ar-5%CO_2	63mm SA387 Gr.11 Cl.1
7	Ar-10%CO_2	63mm SA387 Gr.11 Cl.1
8	Ar-15%CO_2	63mm SA387 Gr.11 Cl.1
9	Ar-20%CO_2	63mm SA387 Gr.11 Cl.1

The original weld, #1, used a 38mm thick 2.25Cr-1Mo pressure vessel steel as a base metal, the first low oxidizing potential weld, #2, was made with the reducing gas mixture and using the same base plate. Slight variations in the welding parameters were required to compensate for arc characteristic changes caused by the composition of the new shielding gas mixture. After completion, the weld specimen was shipped to CANMET for postweld heat treatment and testing. Testing was never carried out due to the fact that the specimen contained through thickness transverse cracks in the weld metal, located approximately every 25mm along the length of the weld. Diffusible hydrogen analysis was then carried out on the electrode and shielding gas combination to determine the amount of weld metal hydrogen produced by the hydrogen content of the shielding gas, Appendix A.

A second weld, #3, was made with the Ar-CO_2-H_2 shielding gas, but due to the nonavailability of the original base metal a

50mm thick SA387 Gr.22 Cl.2 was substituted. Changes in preheat and interpass temperatures, as well as an immediate postweld heat treatment alleviated the cracking problem found in weld #2. Results of subsequent testing indicated that the evaluation of the other shielding gas combinations would be required to optimise the properties of the weld when using the original electrode.

Insufficient amounts of the 50mm base plate and the inability to obtain any other 2.25CR-1Mo forced a change to a 65mm 1.25Cr-0.5Mo (SA387 Gr.11 Cl.1) material as a base metal. Welds were made in the new base plate to duplicate the conditions of welds #1 and #2 to stand as a direct comparison to the welds made with the four other gas mixtures. During the welding of these six specimens the preheat and interpass temperatures of the second Ar-CO_2-H_2(#3) were used for all, however the immediate post weld heat treatment was not given. The procedural details for the welds are given in Table 1.

The six welds were then sent to CANMET for heat treatment, charpy and tensile testing, as well as detailed chemical analysis. Sections of the welds, with no post weld heat treatment, were left at the U. of A. High temperature charpy testing, 100°C, was done to produce completely ductile fracture surfaces for examination by scanning electon microscopy, and to analyse the chemical constituents of the weld metal inclusions.

Although the Twistwire procedure was acceptable for making welds with electrode chemistries supplied by KOBE, there was no flexibility available to vary composition to suit the oxidation

potential of the shielding gas mixtures used. Future experimentation on the interaction of electrode composition and shielding gas oxidation potential depends on easily manipulated electrode chemistry to assess the interaction. Flux-cored and metal powder-cored wires offer the best solution to rapid changes in electrode chemistry. With these wires in mind, a large rotating arc torch was designed and constructed to cope with changes in electrode size, resistivity and composition which is not possible with the single purpose NKK design.

RESULTS

The first noticeable effect of the variations in the oxidizing potential of the shielding gas was the behavior of the welding arc. As the oxidation potential of the shielding gas was lowered, except for the $Ar-CO_2-H_2$ gas, the welding current had to be increased and the arc voltage decreased to maintain suitable arc length and weld profile. While there was no appreciable difference in the appearance of the arc plasma when using the 15 and 20% CO_2 combinations, the 10, 5 and 2% CO_2 shields showed a respectively noticeable deterioration in the stiffness and intensity of the plasma jet, however the operational characteristics of these gases could still be considered as satisfactory. The hydrogen containing gas mixture required only a slight reduction in arc voltage, compared to 20% CO_2, to maintain a suitable arc length, but unlike the straight $Ar-CO_2$ combinations a reduction in welding current was required due to the intensity of the plasma jet which tended to undercut the sidewall if the current was above 500 amperes.

It was also noted at the time of welding that the CO_2 level controlled the amount of silicate and $Mg-O_2$ glass or slag that was left on the surface of the weld bead, the higher oxidation potential gases produced more slag than the low potential gases. Welding fume, a heavy red-brown smoke, was also reduced considerably as the oxidizing potential was lowered.

Weld Metal Residual Elements

All of the welds were analysed for residual oxygen and nitrogen, Table 2, only the procedure using the $Ar-CO_2-H_2$ mixture was analysed for hydrogen. The results of the hydrogen test showed that the shielding gas did not impart sufficient amounts of hydrogen to explain the transverse cracking of weld #2. The hydrogen levels, 2.13 ml/100gm weld metal, are well within the range of a process classified as "good low hydrogen".

Nitrogen levels of the weld metals appeared to be governed by the nitrogen levels of the base plate and the electrode, observed levels of 164-196 ppm were not affected by the oxidation potential of the shielding gas, Figure 2.

Weld metal oxygen levels were definitely controlled by the shielding gas, but also seemed to be affected by the base plate. The original weld, #1, using 80% Ar - 20% CO_2 in the 38mm 2.25Cr - 1Mo plate, was found to have an oxygen content of 520ppm; while the 63mm 1.25Cr -0.5Mo procedure, #9, using the same welding parameters and consumables produced a level of 401ppm. Similar findings came from the two welds made with the $Ar-CO_2-H_2$ gas, #3 and #4. The weld in the 50mm thick 2.25Cr - 1Mo plate contained

165ppm while in the 1.25Cr - 0.5Mo plate levels of 144ppm were obtained. Comparison of the six welds made in the 1.25Cr - 1Mo baseplates shows a definite relationship between the oxidation potential of the gas and the levels of residual weld metal oxygen, Figure 3. The oxidation potential of the $Ar-CO_2-H_2$ gas mixture was determined for the graphical plot by the O_2 content of the weld.

Weld Metal Chemistries

The chemical compositions of the weld metals are given in Table 3. The effects of the oxidizing potential of the shielding gas on the weld metal chemistries was most noticeable in the deoxidant levels, Figure 4. The Mn and Si levels showed an inverse relationship to the weld metal oxygen levels. Weld #1 in the 38mm plate contained 0.68% Mn and 0.24% Si which was comparable to weld #9 in the 63mm plate, 0.675%Mn and 0.25% Si. Weld #3, in the 50mm plate had a radically different analysis than any of the other welds,the chemistry of this weld did not fit or correlate with the trends showed by the other welds, chemical analysis of the baseplate showed 0.52%Mn and only 0.09%Si, which accounts for the differences observed.

In general an increase in the oxidation potential of the shielding gas produced a proportional decrease in the major alloying elements, namely Cr Mo Mn Si, with the greatest effect on Mn and Si. Compared to the 20% CO_2 gas, the 2% CO_2-0.5% H_2 combination caused an increase of 31% in total Mn and Si. This confirms the observations made during the welding procedure that

there was lower slag levels with the lower O_2 potential gases. Welds #4 and #5, 2% CO_2 and 2% CO_2-0.5% H_2, actually had higher Si contents than the electrode. The carbon content also appeared to be controlled by the amount of dilution with the base metal, since the weld carbon contents of welds #4 and #5 were higher than the electrode level but less than that of the baseplate. All other elements showed minimal effects to the oxidation potential.

Inclusion Contents

Scanning electron microscopy was used to examine the failure surfaces of Charpy specimens that were fractured at 100°C to insure a totally ductile fracture surface. Photomicrographs at 3400x magnification were used with 5 random intersects, Figure 5, to determine the average void count for each shielding gas in welds 4 - 9, comparative averages are given in Table 4. Representative photographs are shown in Figures 5A to 5F. An unusual phenomenon was noted on the fracture surfaces of the 2% CO_2 and 2%CO_2-0.5%H_2 welds. Several areas of pico-voids were observed inside the perimeters of micro-voids, Figures 6 and 7 at 2400 and 6400 magnification demonstrate such a site in the 2%CO_2 weld, and Figure 8 at 4900 magnification shows an occurrence in the 2%CO_2-0.5%H_2 weld. Pico-voids were not observed in any of the other weld metals.

Inclusions in the micro-voids were analysed with the S.E.M. and representative spectrum analyses are given in Appendix B. The inclusions from the higher O_2 potential gases were predominantly composed of Fe while the lower oxidizing level gases produced a higher comparative level of alloying elements.

Mechanical Properties

The effects of the higher alloying contents of the weld metals caused the yield and tensile strengths to increase substantially as oxidation potential decreased. Table 5 shows the increase to be sufficient for the yield strength of the Ar-CO_2-H_2 weld to surpass the ultimate strength of the 20% CO_2 weld, 585 and 571 MPa respectively. Five of the welds were remarkably close in ductility, as measured by % elongation and % RA. The only exception was weld #5, which had slightly lower % elongation and % RA than expected. This difference in ductility had no obvious source, but is relevant because Charpy v-notch testing at -40°C showed that weld #5 was the only one to fail the required minimum standard of 54J.

The marked increase in tensile properties were obviously related to the increases in Mn and Si as the residual O levels decreased. The high strength levels adversely affected the fracture toughness, as shown in Table 6. Charpy specimens were extracted at the top of the completed welds (to assess as-deposited microstructures), at the mid-weld depth (to assess typical mixed structures) and at the bottom (to assess root properties). The results show that all of the procedures passed the minimum requirement of 54J in the root areas and in the as-deposited cap pass, but the #5 weld, of lower ductility, did not pass in the mid-depth region. This may be the result of scatter, since individual specimens of the Ar-5%CO_2 and Ar-2%CO_2-0.5%H_2 welds also failed, although the average of three specimens passed. The high alloy level produced from the use of

an electrode wire designed for Ar-20%CO_2 cannot be expected to give good fracture results in comparison with lower strength deposits.

Microstructures

The weld metal microstructures are shown in Figures 9A to 9F. They all show structures apparently of acicular ferrite and some polyganal ferrite. Since it is unlikely that ferrites are formed in a Cr-Mo weld, the ferritic structure observed is probably mostly bainitic in nature. Analysis on a TEM is required to determine the exact nature of the deposits, and will be done in the next phase of the work. The structures are different than similar SAW deposits produced by CANMET, but the alloy levels, especially Mn and Si, are so different that no direct comparison is valid now. The other main observation, again in contrast to SAW results, is that the structure becomes progressively coarser as the residual O level goes down and the Mn and Si levels go up, for example Figure 9F(20CO_2) vs. Figure 9A (2CO_2-.5H_2). This behaviour is similar to that displayed by ferritic weld metals, in which lower transformation temperatures caused by low inclusion contents (nucleation sites for diffusion controlled transformation products) cause a loss of acicular ferrite in the structure and promote bainite. In SAW welds, low residual O levels promote finer microstructures, but these welds do not have the Mn-Si levels, and high O SAW deposits have low C levels compared to GMAW deposits, 0.06% vs. 0.10%.

The new rotating arc torch constructed to use single wire electrodes is described in detail in Appendix C. So far it has

been used only to deposit bead-on-plate runs using CONARCO 1.6mm diameter experimental Cr-Mo powder-cored electrodes. The first batch of two reels showed that excessive porosity was developed during deposition. However, this problem was traced to an influx of air into the shielding gas stream. When this problem was corrected, the wires ran very well in a shielding gas of $Ar-2\%CO_2-0.5\%H_2$. There was a significant amount of slag left on the bead surface in spite of the low oxidation potential of the shielding gas, which CONARCO is addressing for the second batch of electrodes by reducing the amount of slag-formers in the core. The question of the correct amount of slag-formers and the balance of deoxidants for low oxidation potential shielding gases is the outstanding problem to be addressed before mechanical property determination can be started on the next generation of GMAW narrow-gap welds. CONARCO is now committed to refining the slag-former and alloy balance during the remainder of the contract.

DISCUSSION

The results show clearly that weld metal oxygen content, and therefore the total inclusion level, can be closely controlled (for a given base metal and electrode wire combination) via the oxidation potential of the shielding gas. Adding hydrogen to the gas does not appear to reduce O further, but the associated increases in Mn and Si levels suggest that the oxidation potential of the gas is reduced. A possible answer is that base metal dilution is a significant factor at low O levels, and the shielding gas will not have a substantial effect on base metal O,

since the bulk of gas-metal reactions take place at the electrode tip.

The high Mn and Si levels produced with low oxidation potential shielding gases are both unnecessary and detrimental to toughness in these weld metals. Electrode wire compositions for GMAW procedures need to be "tuned" to the shielding gas in much the same way that SAW wires and fluxes are designed for each other. The most efficient way to do this is to use metal powder cored wires with low but sufficient deoxidizing power to produce minimal O levels with adequate alloy levels for the desired application. The low O levels will definitely improve ductile fracture characteristics, and the results produced here strongly suggest that low temperature toughness would also be improved.

CONCLUSIONS

1. Modification of the oxidation potential of the shielding gas controls the residual O content of narrow-gap GMAW procedures. Slight changes are necessary in the procedure with respect to volts, amperes and welding speed, but nothing substantive.
2. The use of low CO_2 and additions of H_2 to the shielding gas produces a reduction in residual O content by a factor of three, e.g. from 400 to 140 ppm. However, electrode wires designed for high CO_2 levels in the shielding gas produce weld metals high in Mn and Si, increasing the strength and impairing fracture toughness.
3. GMAW electrodes and shielding gases could benefit by being designed as complementary to each other, as are SAW consumables.
4. Metal powder cored wires with minimal deoxidant levels offer the best solution to complementary GMAW consumables, due to the difficulty of easily changing the chemical composition of solid wires. The new rotating arc technology will provide the best opportunity to use powder-cored wires, since twistwire technology involves an unacceptable deformation of tubular wires, causing wire kinking and instability.

REFERENCES

1. **B.H. Baker, N. Crevis, J.A. Lucey & F.W. Lunau** *"Mild Steel Welding with Argon/CO_2 Mixtures"*
British Welding Journal x (4) p627 1961

2. **B.M. Patchett & A.C. Bicknell** *"Narrow Gap Welding of C-Mn and Cr-Mo Steels"*
Welding Engineering Report #5, University of Alberta, April 1985

3. **R. Chandel, R.F. Orr, J.A. Gianetto, J.T. McGrath, B.M. Patchett & A.C. Bicknell** *"The Microstructure and Mechanical Properties of Narrow Gap Welds in 2.25Cr - 1Mo Steel"*
IIW Document IX-1355-85 1985

Table 1

Weld #	Volts	Amps	Speed	Minimum Preheat-° C	Maximum Interpass-° C	PWHT*
1	30.0	500	250	150	200	None
2	28.5	480-500	230-250	150	200	None
3	28.5	480-500	230-250	200	225	9 hrs @ 685°C
4	28.5	480-500	230-250	200	225	None
5	27.0	520	230-250	200	225	None
6	27.0	500-520	230-250	200	225	None
7	28.0	500-520	230-250	200	225	None
8	29.0	500	230-250	200	225	None
9	29.0	500	230-250	200	225	None

*Post Weld Heat Treatment: Immediately after welding, prior to shipment to P.M.R.L.

Table 2 - Weld Metal Residual Gas Levels

Weld #	Shielding Gas % Carbon Dioxide	% Hydrogen	Base Metal	Oxygen PPM	Nitrogen PPM
1	20		38 mm 2 1/4 Cr-1 Mo	520	-
3	2	0.5	50 mm 2 1/4 Cr-1 Mo	169	160
4	2	0.5	63 mm 1 1/4 Cr-1/2 Mo	144	187
5	2		63 mm 1 1/4 Cr-1/2 Mo	149	182
6	5		63 mm 1 1/4 Cr-1/2 Mo	215	184
7	10		63 mm 1 1/4 Cr-1/2 Mo	302	196
8	15		63 mm 1 1/4 Cr-1/2 Mo	370	179
9	20		63 mm 1 1/4 Cr-1/2 Mo	401	185

Table 3 - Chemical Compositions, Wt %

Material	C	Mn	Si	S	P	Ni	Cr	Mo	Al	O
TWS - 2 CM	0.080	0.960	0.330	0.009	0.004	0.15	2.33	1.080	-	-
38 mm plate	0.100	0.490	0.200	0.028	0.008	0.33	2.27	1.030	0.010	-
50 mm plate	0.140	0.520	0.090	0.003	0.004	0.02	0.26	1.040	0.017	-
63 mm plate	0.130	0.510	0.520	0.014	0.006	0.21	1.3	0.490	-	-
Weld #1	0.090	0.680	0.240	0.013	0.006	0.20	2.22	1.030	0.010	0.0520
Weld #3	0.140	0.580	0.230	0.005	0.006	0.13	2.35	1.040	0.028	0.0169
Weld #4	0.100	0.860	0.350	0.010	0.005	-	2.19	1.000	0.005	0.0144
Weld #5	0.105	0.830	0.345	0.010	0.005	-	2.14	0.980	0.005	0.0149
Weld #6	0.110	0.810	0.315	0.010	0.006	-	2.15	0.985	0.004	0.0215
Weld #7	0.110	0.715	0.310	0.010	0.006	-	2.09	0.920	0.003	0.0302
Weld #8	0.105	0.685	0.280	0.010	0.006	-	2.07	0.945	0.003	0.0370
Weld #9	0.110	0.675	0.250	0.010	0.006	-	2.11	0.980	0.004	0.0401

Table 4 - Fracture Surface Void Sizes

Weld #	Figure #	Shielding Gas % Carbon Dioxide	% Hydrogen	Magnification	Average Void Size
9	5A	20		3400	2.16 µm
8	5B	15		3400	2.15 µm
7	5C	10		3400	2.27 µm
6	5D	5		3400	2.64 µm
5	5E	2		3400	2.79 µm
4	5F	2	0.5	3400	3.16 µm

Table 5 - Mechanical Properties

Weld #	Shielding Gas		Yield Stress	Ultimate Stress	% Elongation	% RA
	% Carbon Dioxide	% Hydrogen	MPa	MPa		
9	20		489	571	24	69
8	15		501	576	24	72
7	10		503	577	23	73
6	5		535	600	23	72
5	2		574	634	20	58
4	2	0.5	585	647	23	71

Table 6 - Charpy Impact Results

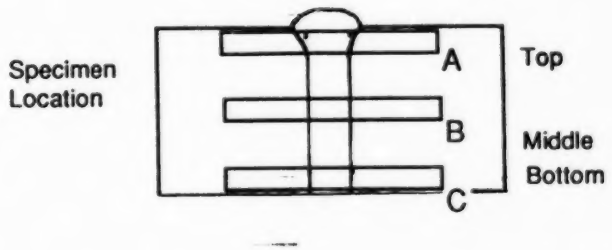

Weld #	Test Tem. °C	A Joules	B Joules	C Joules
4	-40	124, 98, 82	42, 71, 63	11, 15, 70
	25	202	-	-
5	-40	60, 105, 93	20, 33, 60	60, 57, 122
	25	197, 232	194, 148	203, 196, 196
6	-40	152, 169, 151	125, 93, 39	77, 38, 143, 120
	25	245, 230, 228	180, 188	198, 230, 194, 210
7	-40	131, 120, 126	122, 63, 34	97, 26, 38
	25	142, 170, 240, 235	184, 214, 185	176, 176
8	-40	86, 88, 112	76, 93, 40	77, 93, 35
	25	153, 182	164	164, 166, 166
9	-40	71, 77, 71	72, 78, 84	91, 43, 23
	25	-	-	162, 192

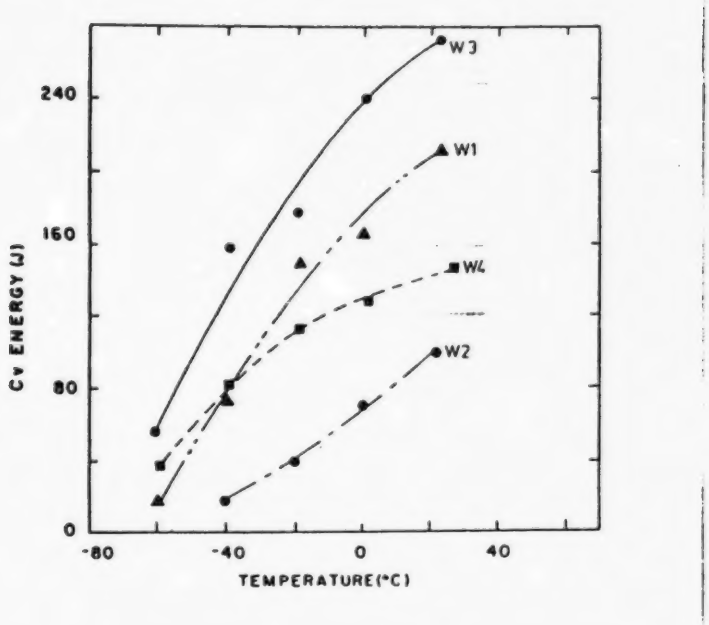

Figure 1. Charpy impact transition curves for narrow gap welds from E.M.R. comparison

		Volume Fraction of Inclusions	Weld Metal $S + O_2$
W3	SAW	0.40%	0.029%
W1	SAW	0.48%	0.035%
W4	GMAW	0.50%	0.065%
W2	SAW	0.96%	0.096%

FIGURE 2.

OXYGEN – NITROGEN CONTENT

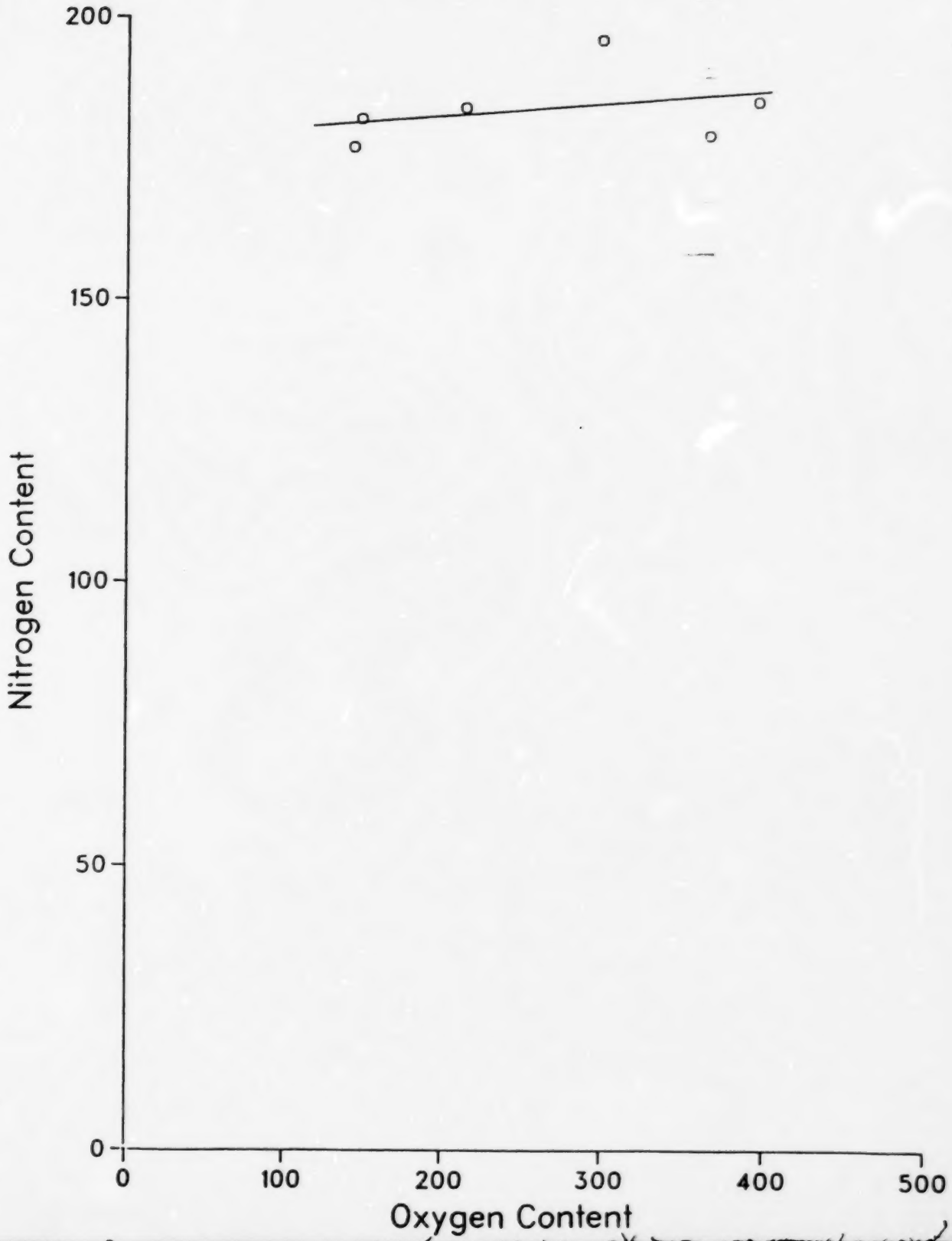

FIGURE 3.

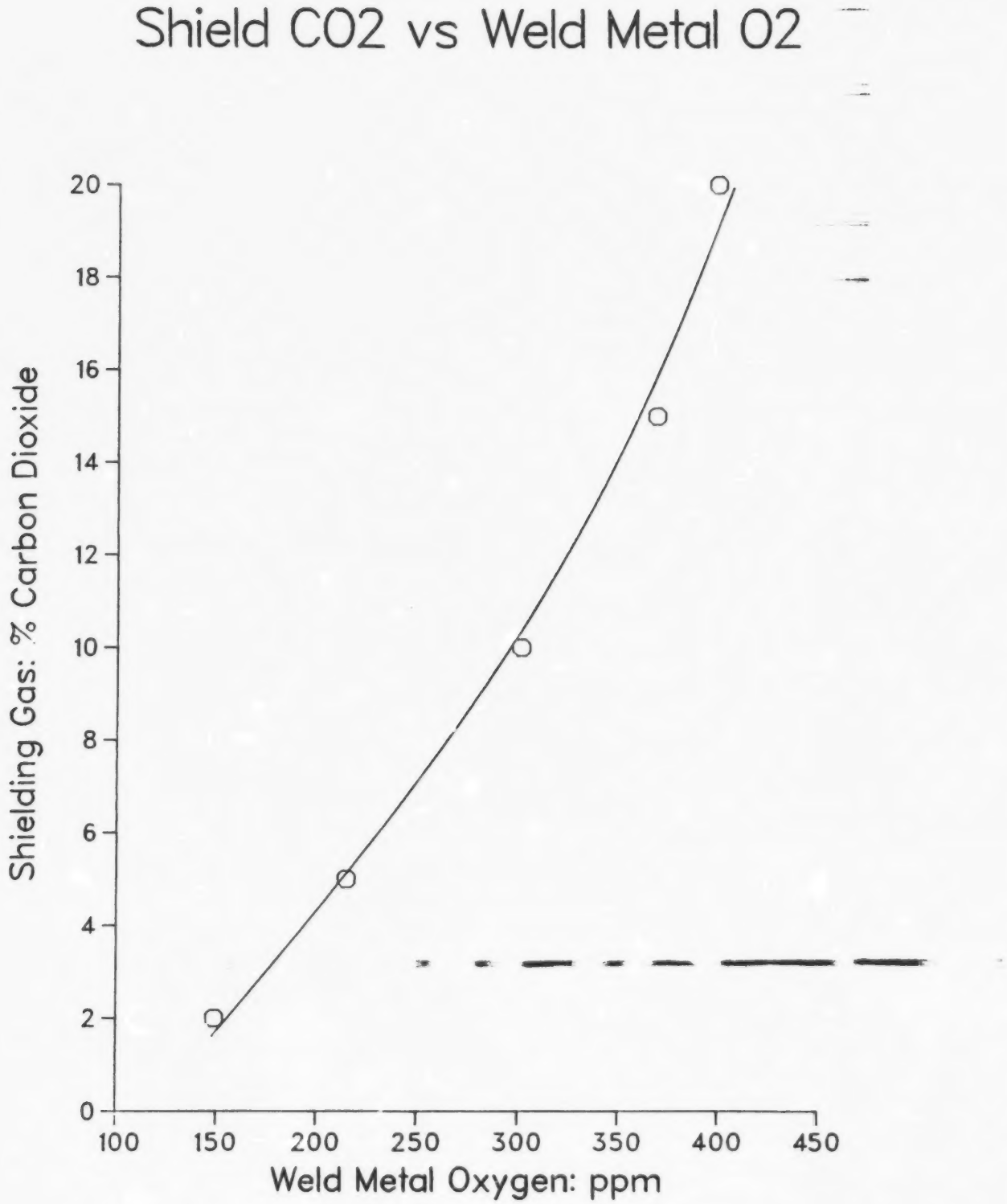
Shield CO2 vs Weld Metal O2
Shielding Gas: % Carbon Dioxide
0
2
4
6
8
10
12
14
16
18
20
100
150
200
250
300
350
400
450
Weld Metal Oxygen: ppm

FIGURE 4.

Weld Metal O2 vs Weld Metal Deoxidants

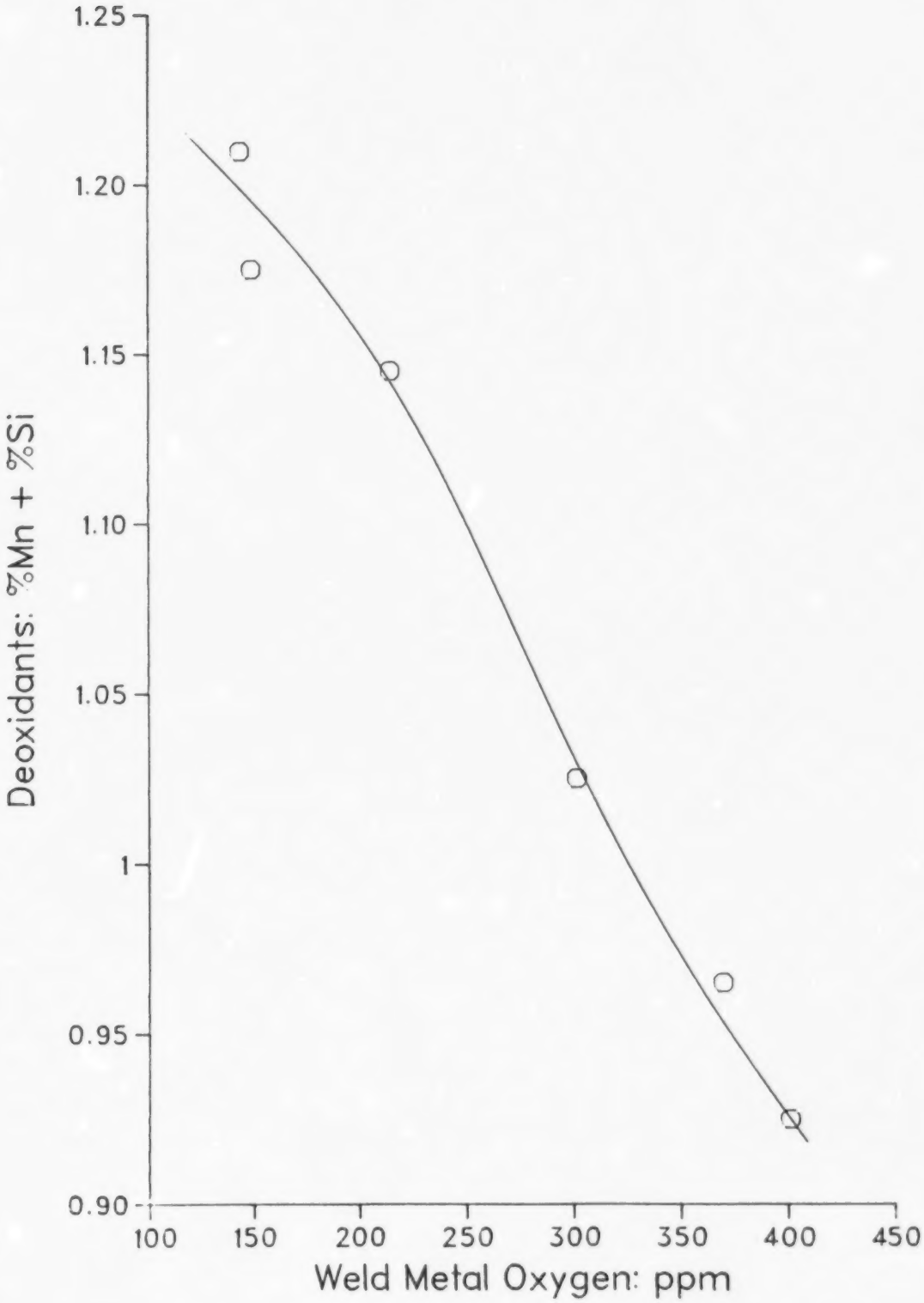

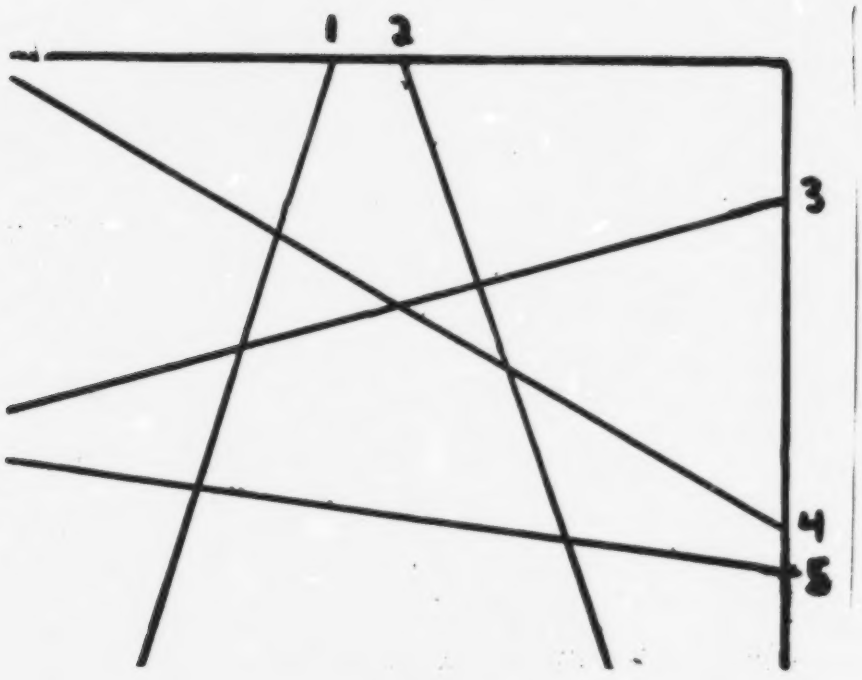

Figure 5. Random Intersepts for Void Sizing

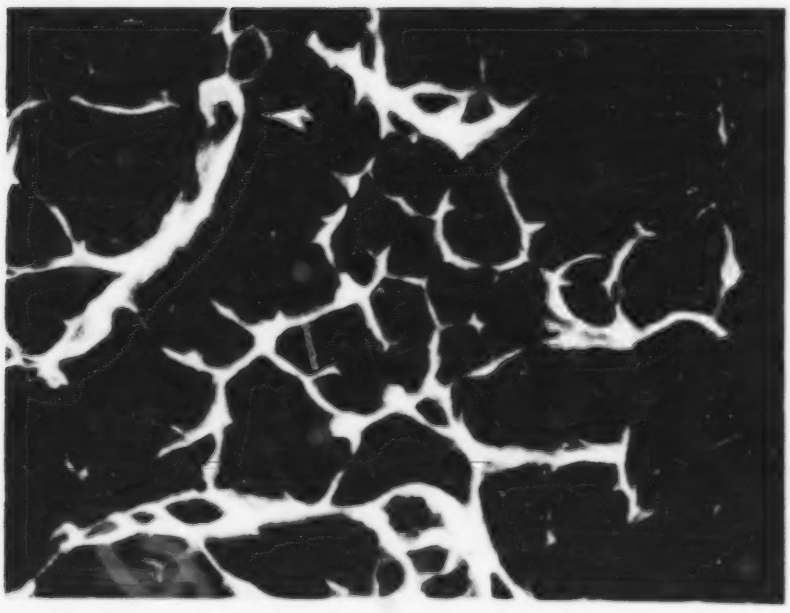

Figure 5A. Fracture Surface Weld #9 - 3400X

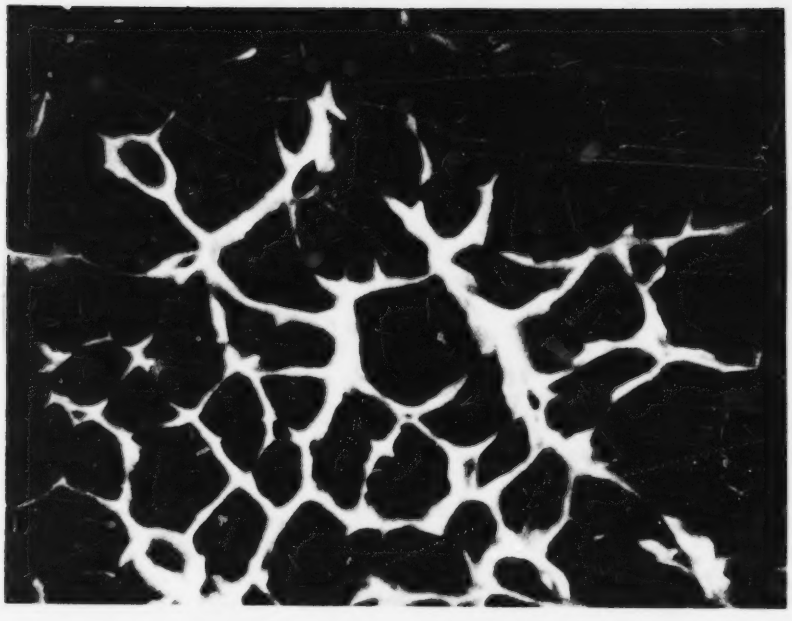

Figure 5B. Fracture Surface Weld #8 - 3400X

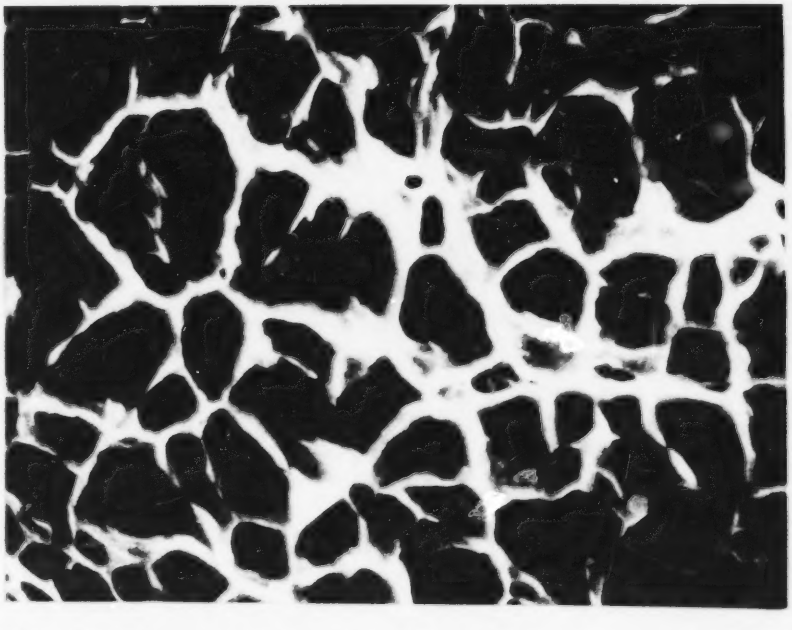

Figure 5C. Fracture Surface Weld #7 - 3400X

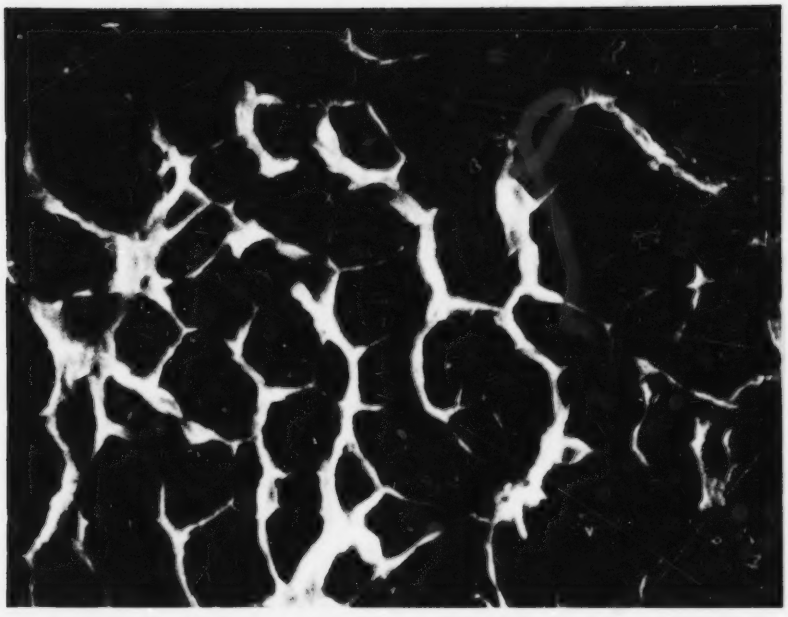

Figure 5D. Fracture Surface Weld #6 - 3400X

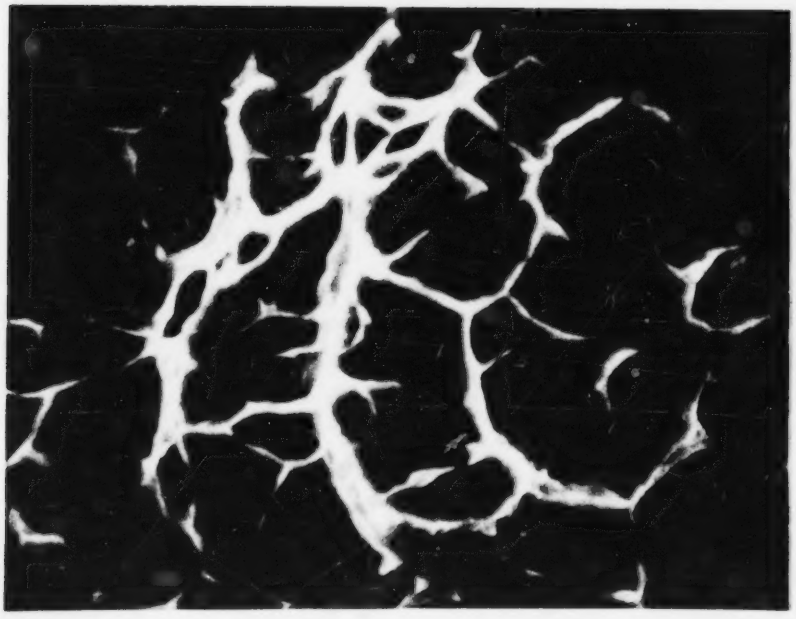

Figure 5E. Fracture Surface Weld #5 - 3400X

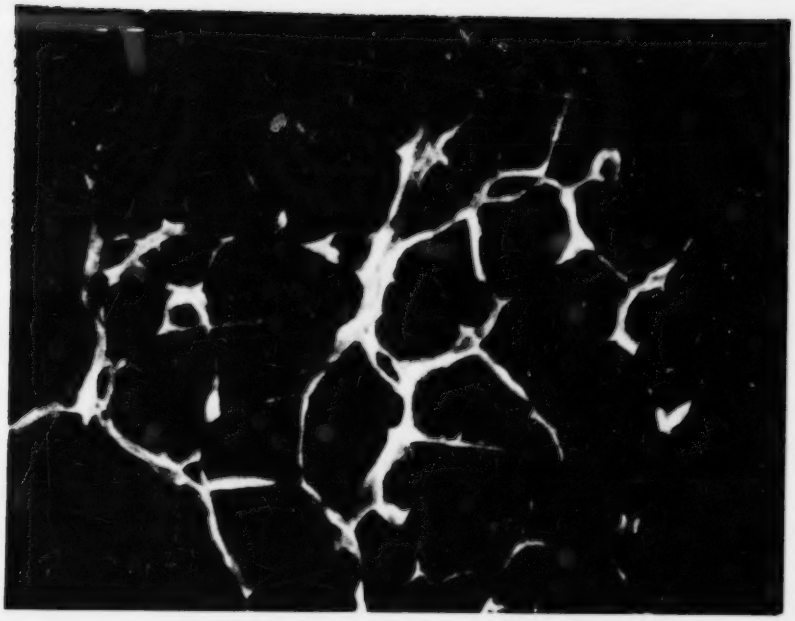

Figure 5F. Fracture Surface Weld #4 - 3400X

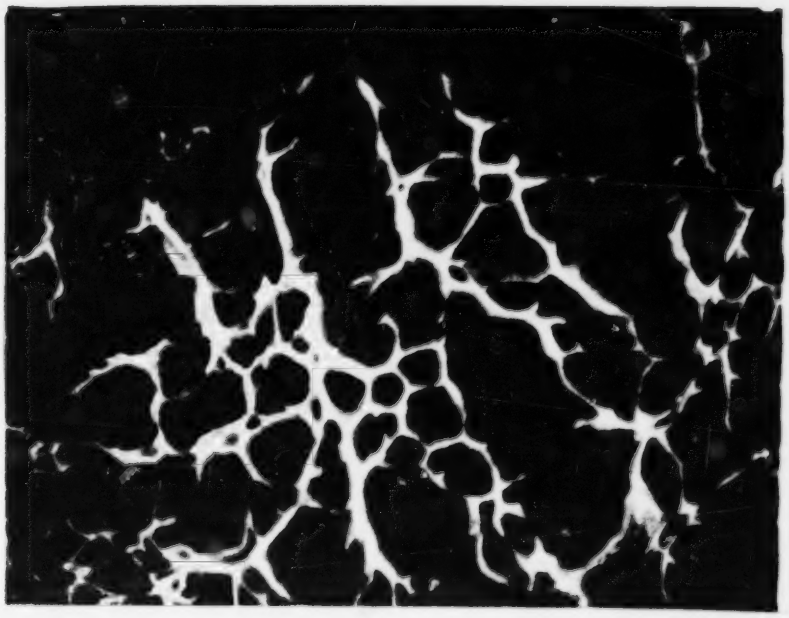

Figure 6. Picovoids Weld #5 - 2400X

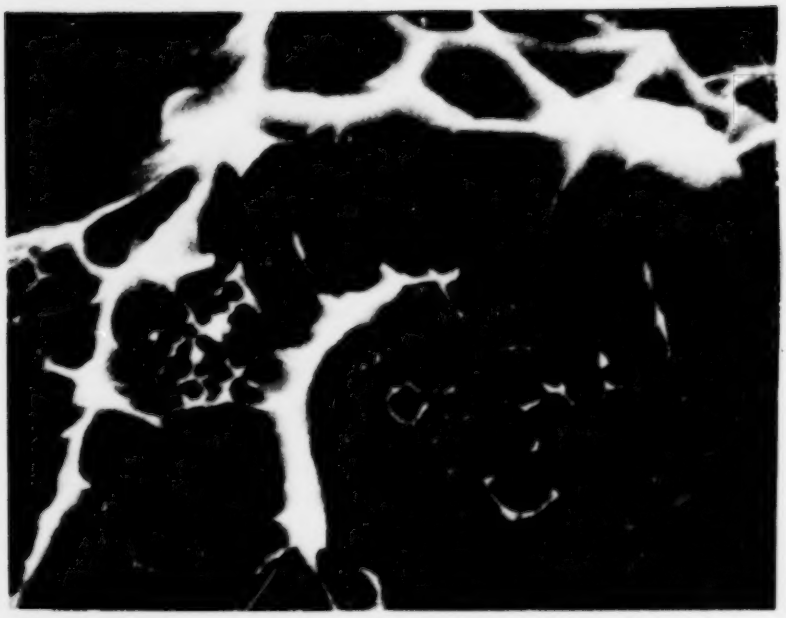

Figure 7. Picovoids Weld #5 - 6400X

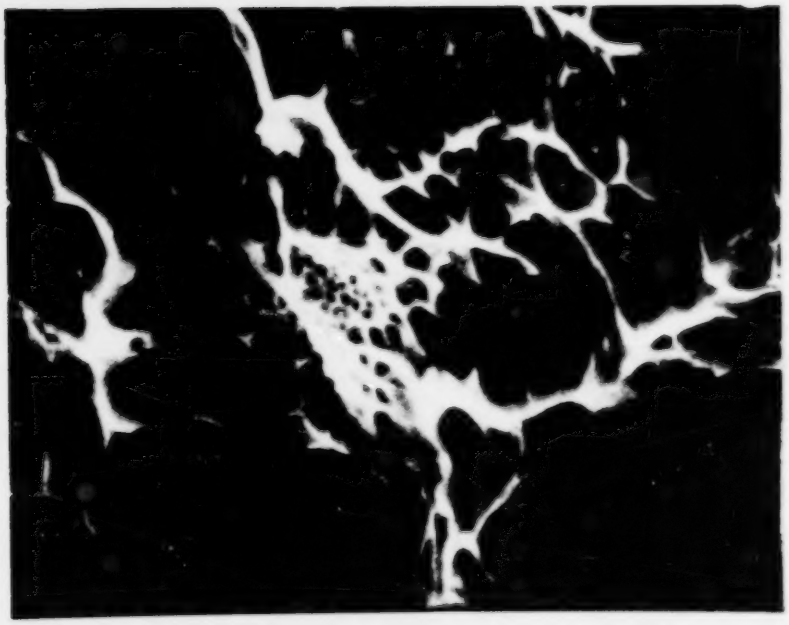

Figure 8. Picovoids Weld #4 - 4900X

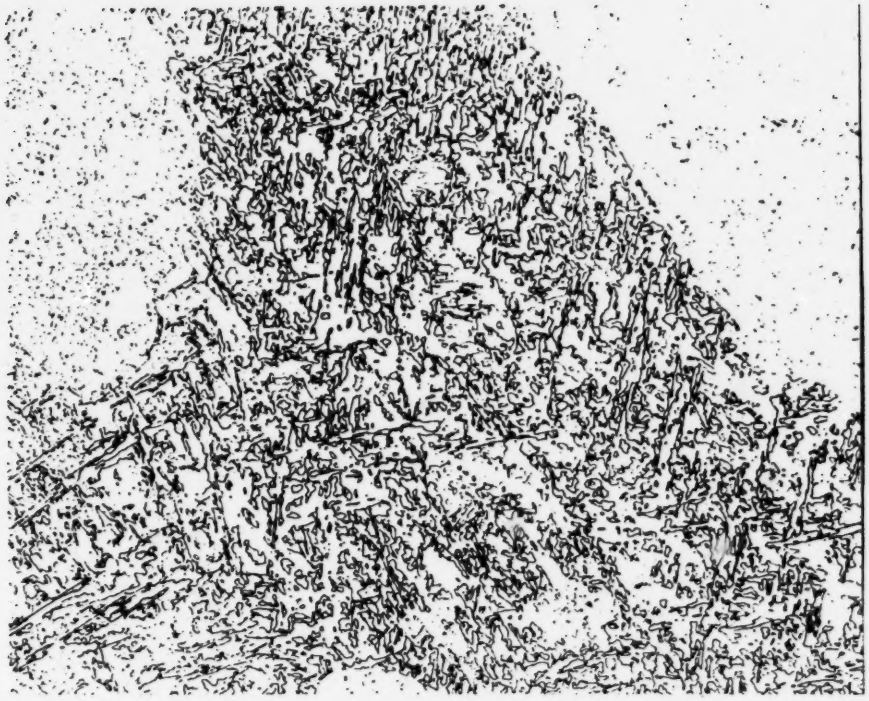

Figure 9A. Microstructure Weld #4

Figure 9B. Microstructure Weld #5

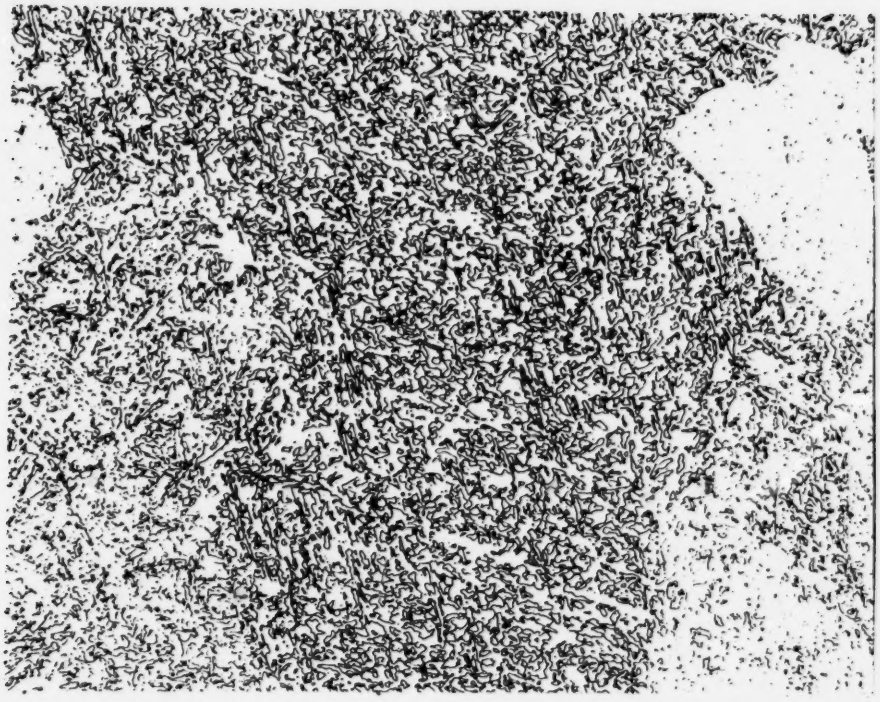

Figure 9C. Microstructure Weld #6

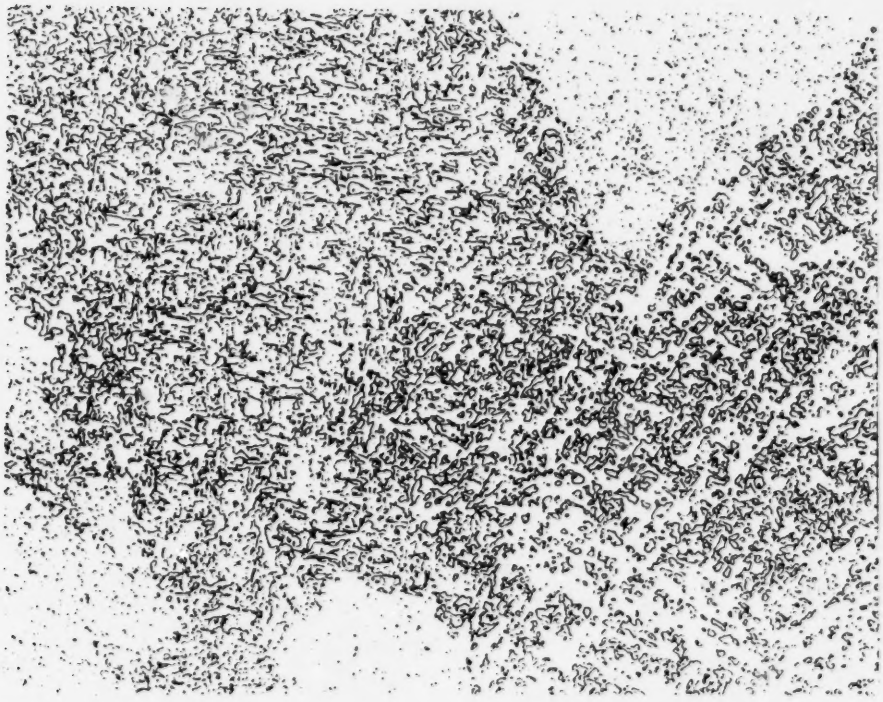

Figure 9D. Microstructure Weld #7

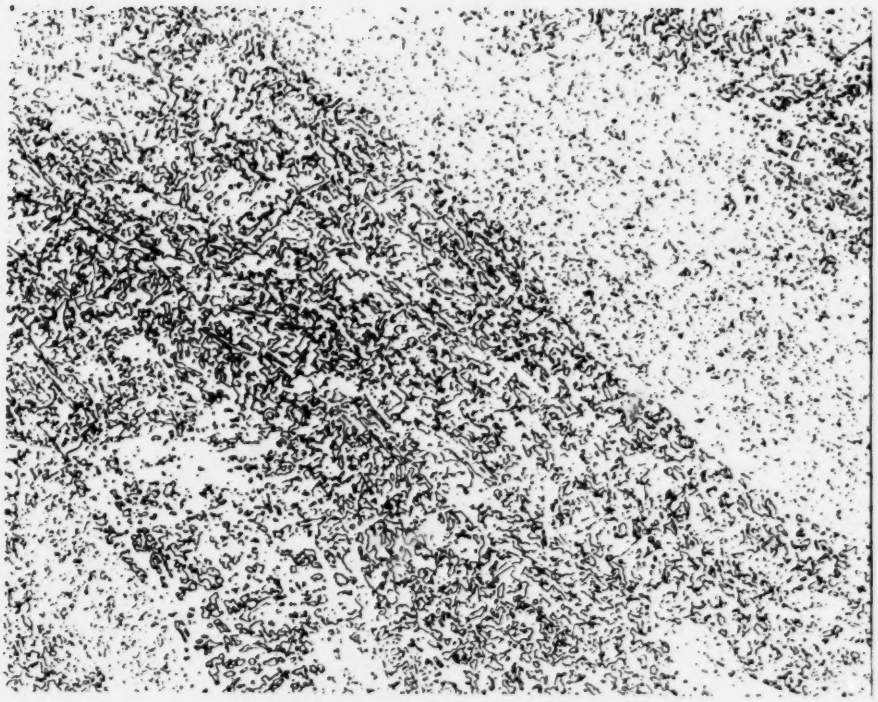

Figure 9E. Microstructure Weld #8

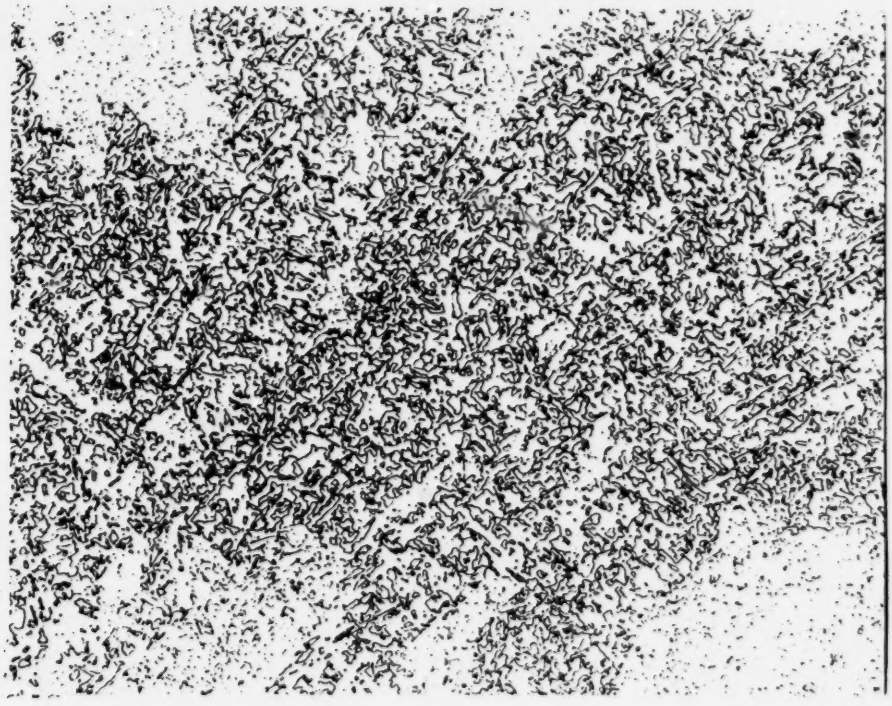

Figure 9F. Microstructure Weld #9

APPENDIX A

UNIVERSITY OF ALBERTA

DEPARTMENT OF MINERAL ENGINEERING

FCAW/GMAW HYDROGEN TEST

DATE _____

WELDER C. Bicknell CUSTOMER P.M.R.L.

ELECTRODE MANUFACTURER KOBE

ELECTRODE CLASS TWS-2CM BATCH NO. 31061-7926

ELECTRODE DIA. 2 x22mm mm FEED RATE ---------- m/min

FUSED ZONE LENGTH --------- mm WELDING SPEED 250 mm/min

SHIELDING GAS COMPOSITION 97.5 %Ar --- %He 2.0 $\%CO_2$ ---- $\%O_2$

0.5 $\%H_2$ -- % -- % -- %

FLOW RATE 50 + 50 l/min

ARC TIME ---------- sec STICKOUT 35 mm

CURRENT 500 amps. VOLTAGE 30 volts

CURRENT TYPE D.C. ELECTRODE POLARITY POS.

HYDROGEN CONTENT ppm _____ AVERAGE _____ PEAK

ml/100gm 2.14 AVERAGE 2.22 PEAK

APPENDIX A

UNIVERSITY OF ALBERTA

DEPARTMENT OF MINERAL ENGINEERING

WELDING LABORATORY

WELD METAL HYDROGEN ANALYSIS

Wgt. of Test Piece & Weld Metal	45.4730	gm
Wgt. of Test Piece	36.9596	gm
Wgt. of Weld Metal	8.5134	gm
Fused Metal Area	-----	mm^2
Deposited Metal Area	-----	mm^2
Hydrogen Collection Temperature	22	^oC
Hydrogen Collection Time	96	hr
Barometric Pressure = P	698.7	mm Hg
Ambient Temperature = T	22	^oC
Length of Hydrogen Column = L	2.3	cm
Head of Mercury on Capillary = H	201	mm
Diameter of Capillary = d	0.4	cm

$$V_H = 4.5 \times 10^{-2} \frac{(P-H)(L)}{(273+T)} = .175 \text{ ml}$$

= 2.05ml/100g

APPENDIX A

UNIVERSITY OF ALBERTA

DEPARTMENT OF MINERAL ENGINEERING

WELDING LABORATORY

WELD METAL HYDROGEN ANALYSIS

Wgt. of Test Piece & Weld Metal	44.6235	gm
Wgt. of Test Piece	37.0754	gm
Wgt. of Weld Metal	7.5481	gm
Fused Metal Area	-------	mm^2
Deposited Metal Area	-------	mm^2
Hydrogen Collection Temperature	22	^oC
Hydrogen Collection Time	96	hr
Barometric Pressure = P	698.7	mm Hg
Ambient Temperature = T	22	^oC
Length of Hydrogen Column = L	2.09	cm
Head of Mercury on Capillary = H	173	mm
Diameter of Capillary = d	0.4	cm

$$V_H = 4.5 \times 10^{-2} \frac{(P-H)(L)}{(273+T)} = .168 \text{ ml}$$

$$= 2.22 \text{ml}/100\text{g}$$

APPENDIX B

SPECTRUM ANALYSES

OF

MICROVOID INCLUSIONS

IN

2¼ Cr - 1 Mo WELD METAL

INCLUSION(20% CARBON DIOXIDE)

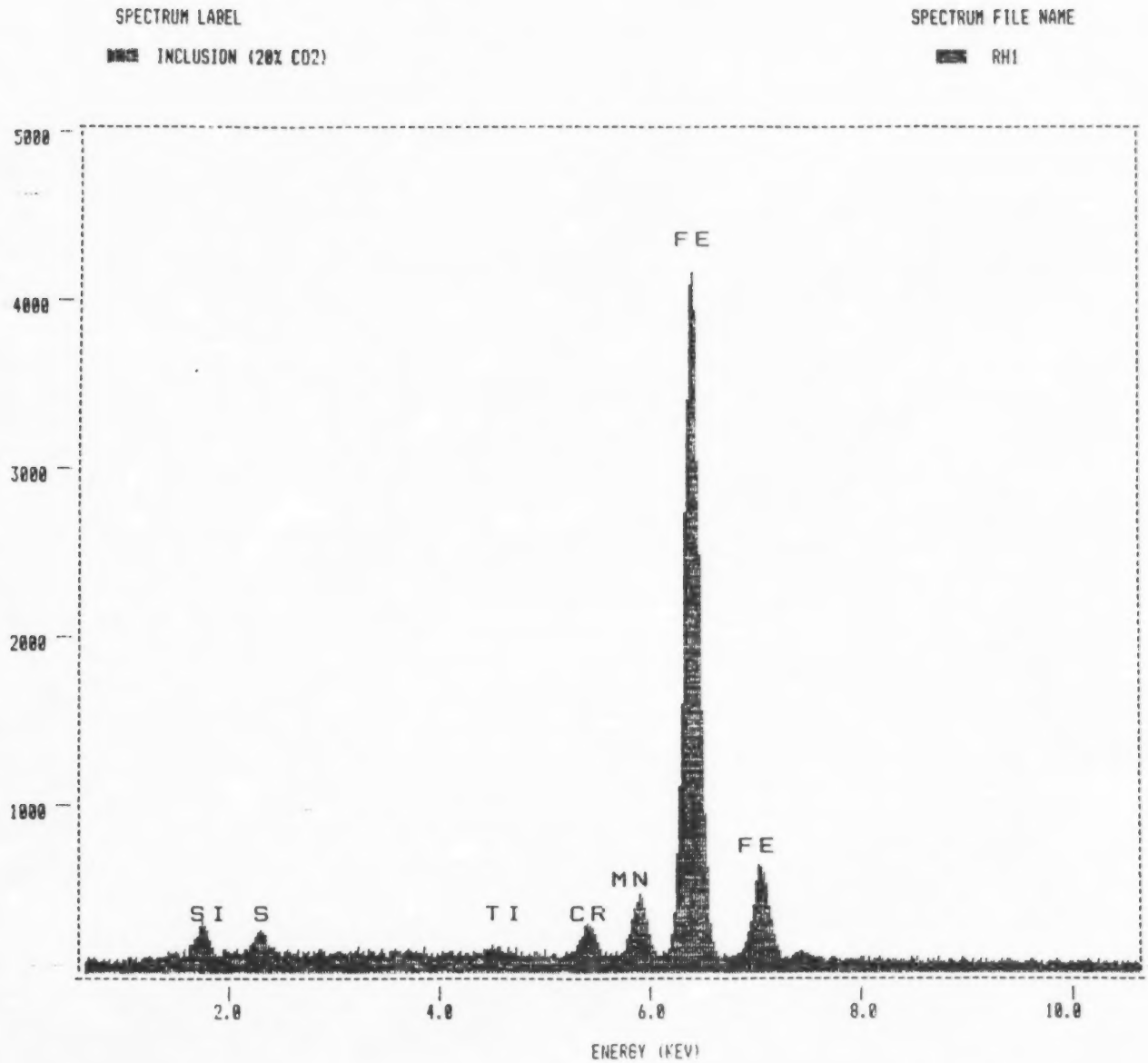

PIGIT

INCLUSION(15% CARBON DIOXIDE)

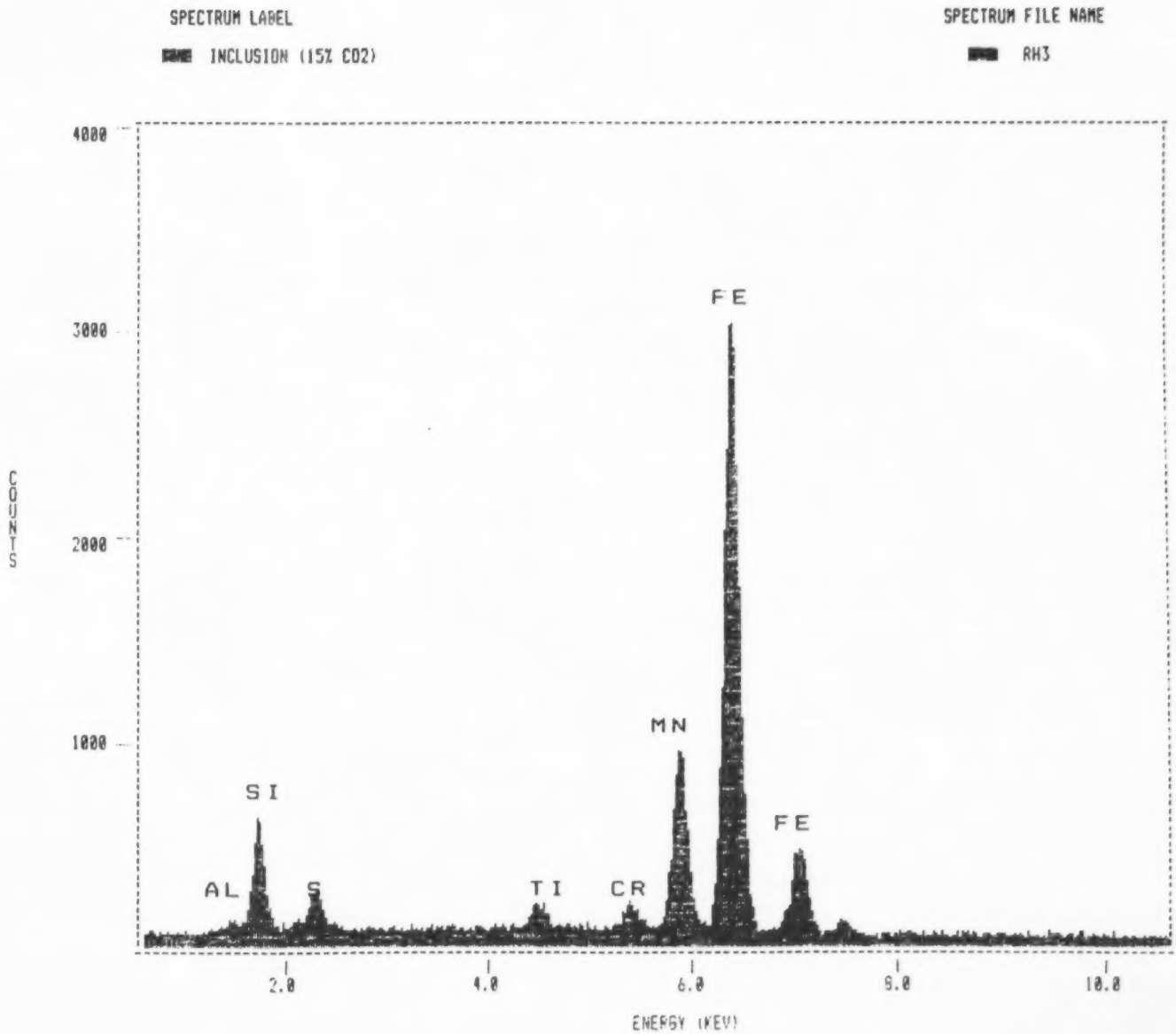

FIGURE

INCLUSION(10% CARBON DIOXIDE)

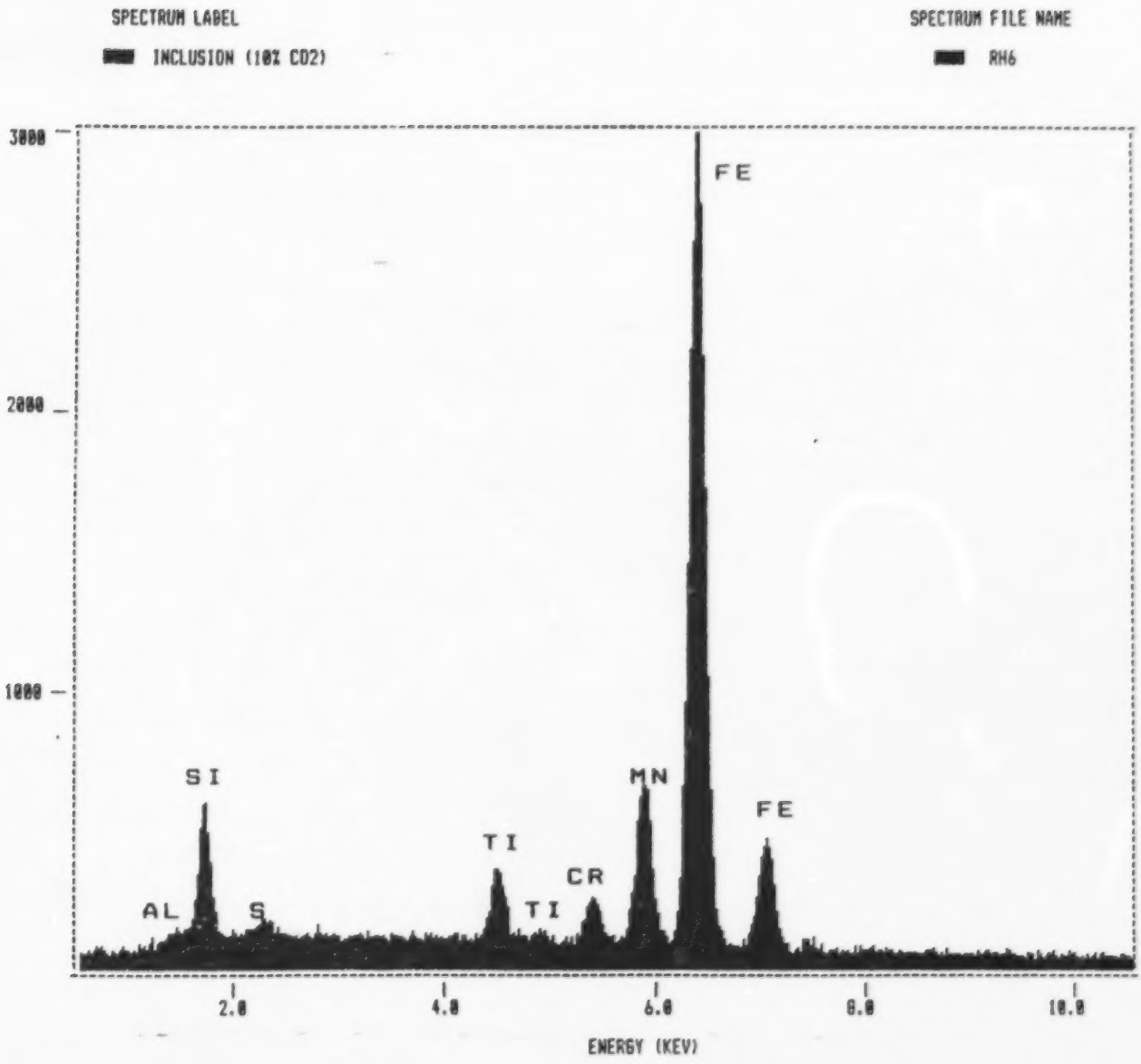

PIGITI

INCLUSION(5% CARBON DIOXIDE)

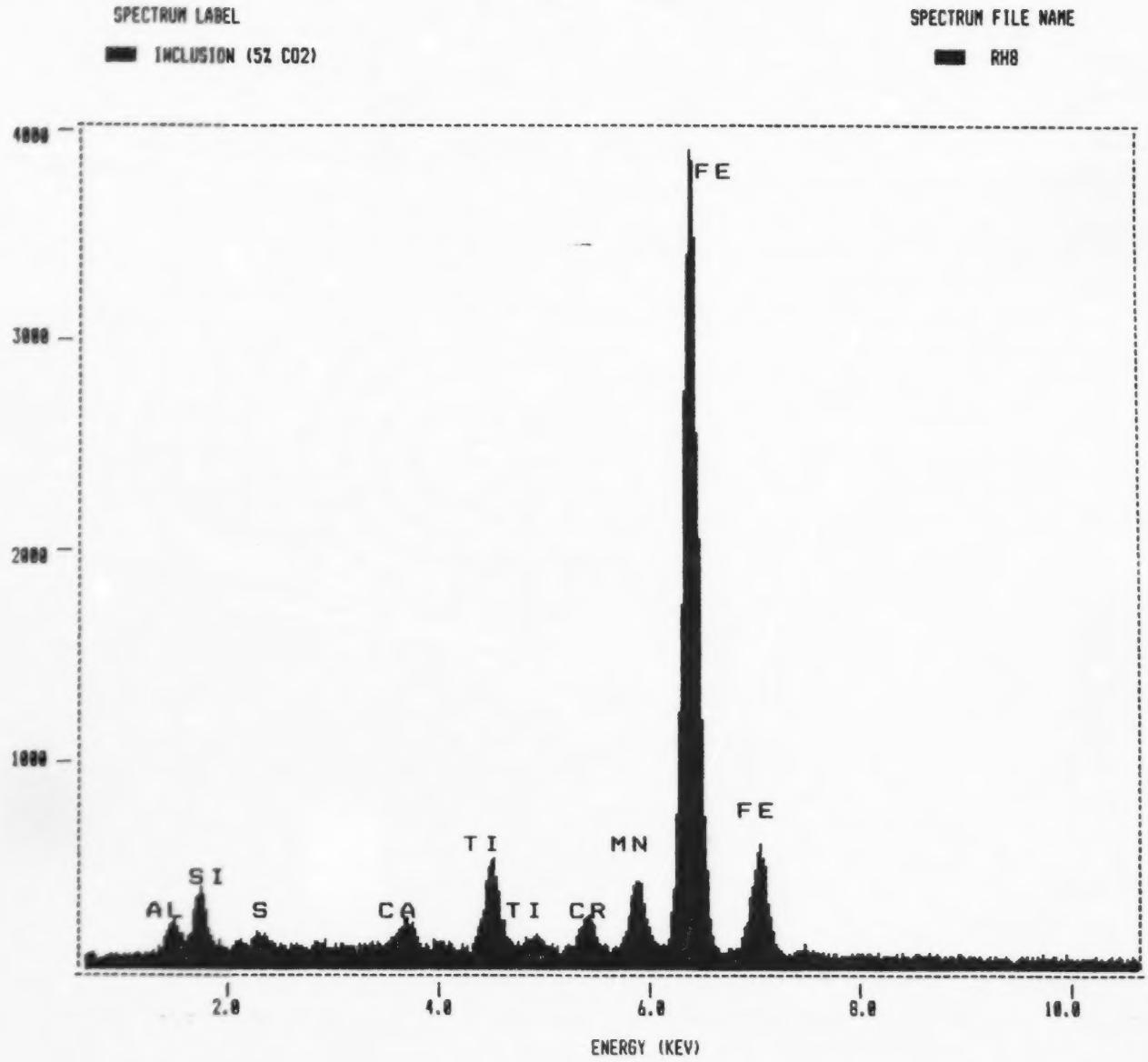

PIGIT

INCLUSION(2% CARBON DIOXIDE)

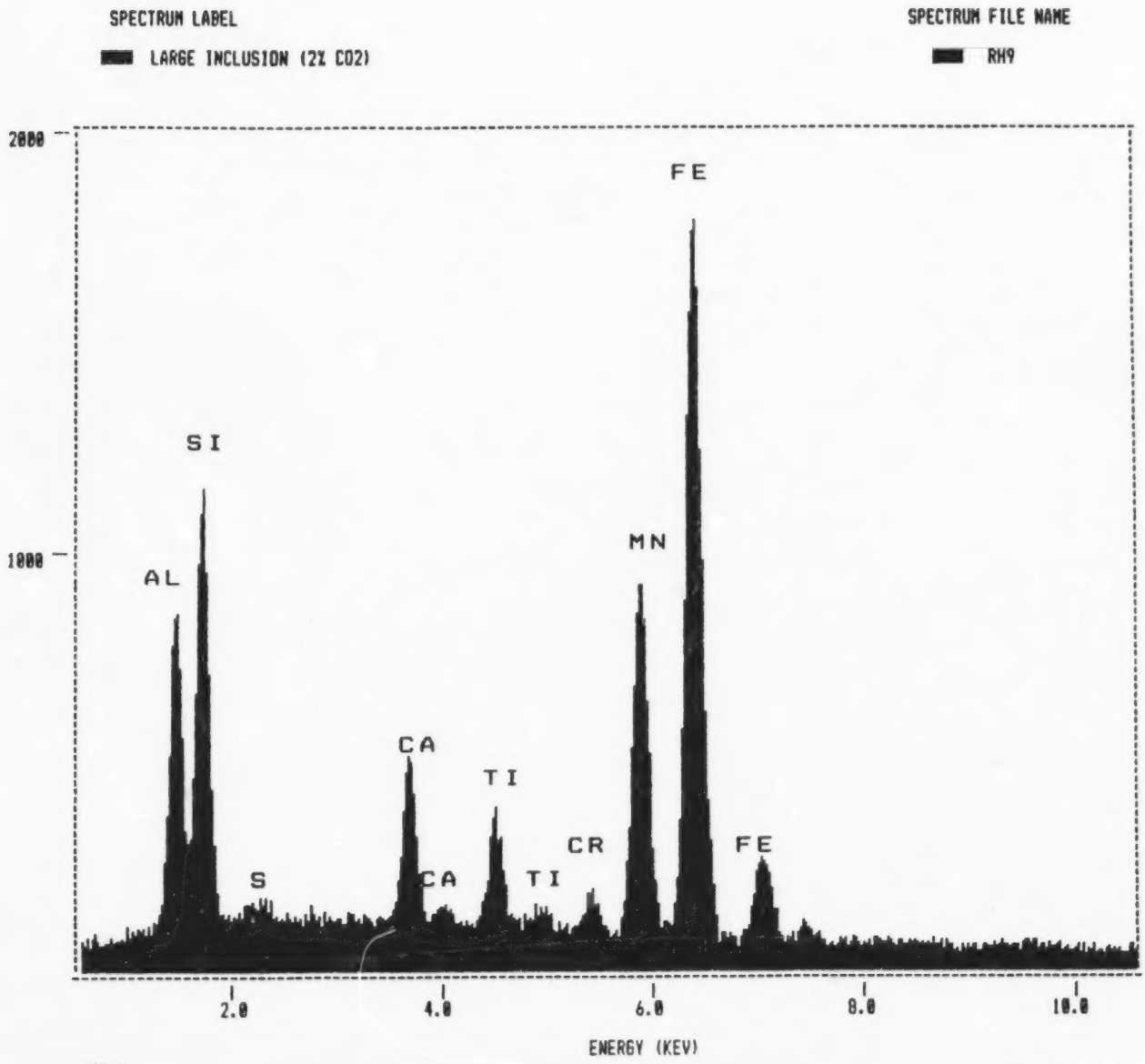

PIGITI

INCLUSION (2% CO_2 + 0.5% H_2)

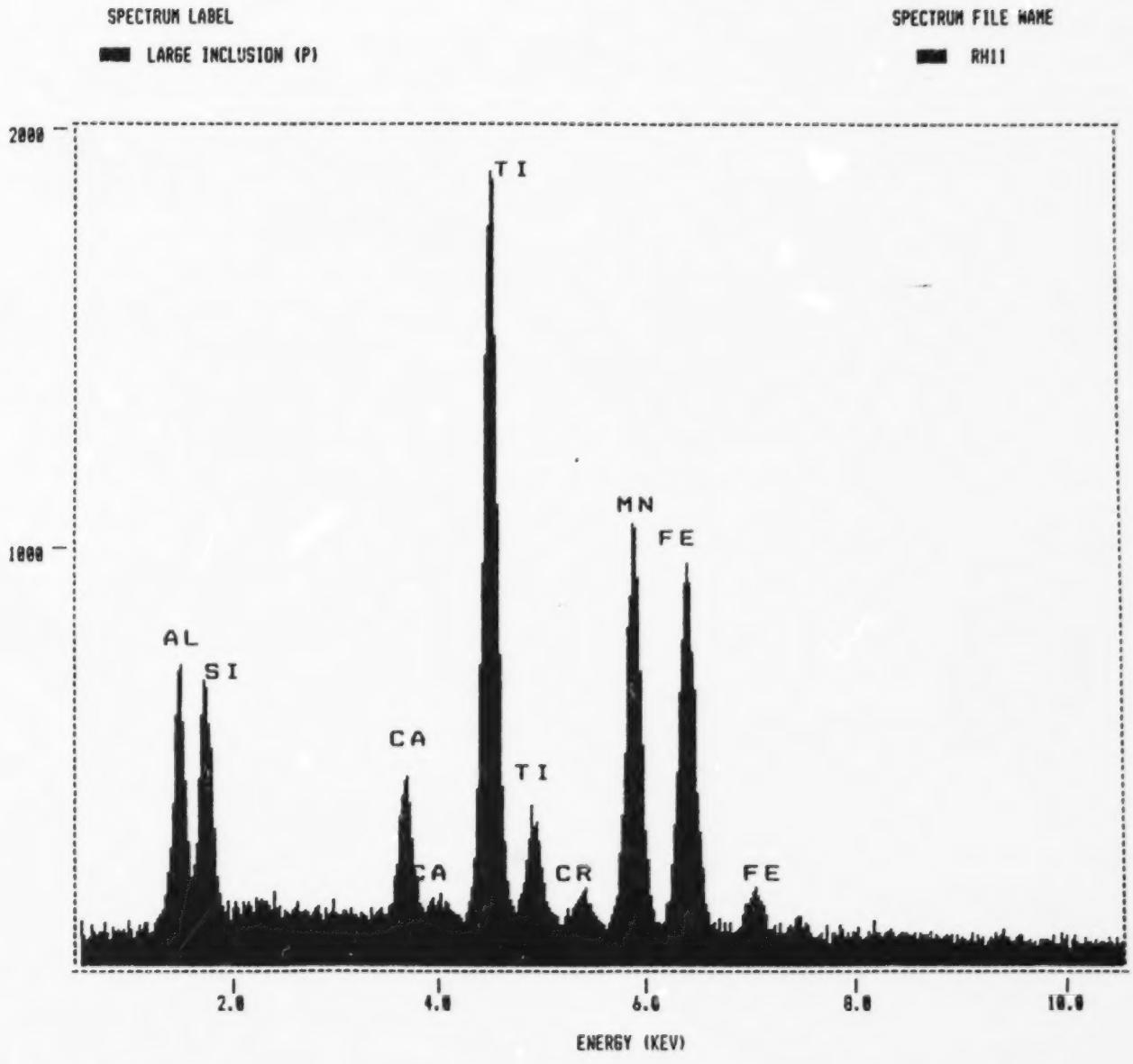

PIGITI

APPENDIX C

The experimental rotating arc torch was designed using the principles developed by NKK for their rotating arc machine, but modified for the following purposes:

1. Use of variable currents to avoid the restriction of only two wire diameters (1.2 and 1.6mm) which must be solid carbon or stainless steel. The NKK machine uses a synergic power source which uses stickout resistivity to control torch positioning and power output during welding. Therefore changes in wire diameter and composition can cause significant instabilities if the machine settings are unable to accommodate the diameter/resistivity relationship.
2. Use of higher or lower currents to accommodate both flux-cored and powder-cored wires and smaller diameter wires respectively. Flux-cored and powder-cored wires often have different penetration characteristics in comparison with solid wires and need differing currents as a result.

The detailed design of the torch is shown in Figure C1. The NKK torch body utilizes a single carbon (copper impregnated) circular brush to transmit the welding current from a fixed vertical brush to the rotating brass contact plate and torch mechanism. The new design uses six horizontal graphite brushes 25mm in diameter to transmit current to the vertical brass cylindrical transition piece between the geared rotating mechanism and the tubular welding torch. The rotating mechanism also differs from the NKK system. The NKK machine uses step-up gearing to produce a rotational frequency of 100 Hz maximum from

a 50 Hz DC motor. Originally, the new torch used an AC motor and step-up gearing as well. However, the drag of the six graphite brushes stalled the AC motor, despite its higher power compared to the NKK motor. The motor and gearing system was altered to use a DC motor of slightly higher power (250 vs 200 W) and a step-down gearing (from 100 Hz to 60 Hz maximum) to take advantage of the extra torque available in a high speed motor. Most welding procedures developed by NKK use a optimum rotating frequency of 50 Hz, suggesting that the maximum frequency reduction of the new torch will not be a significant handicap for procedure development.

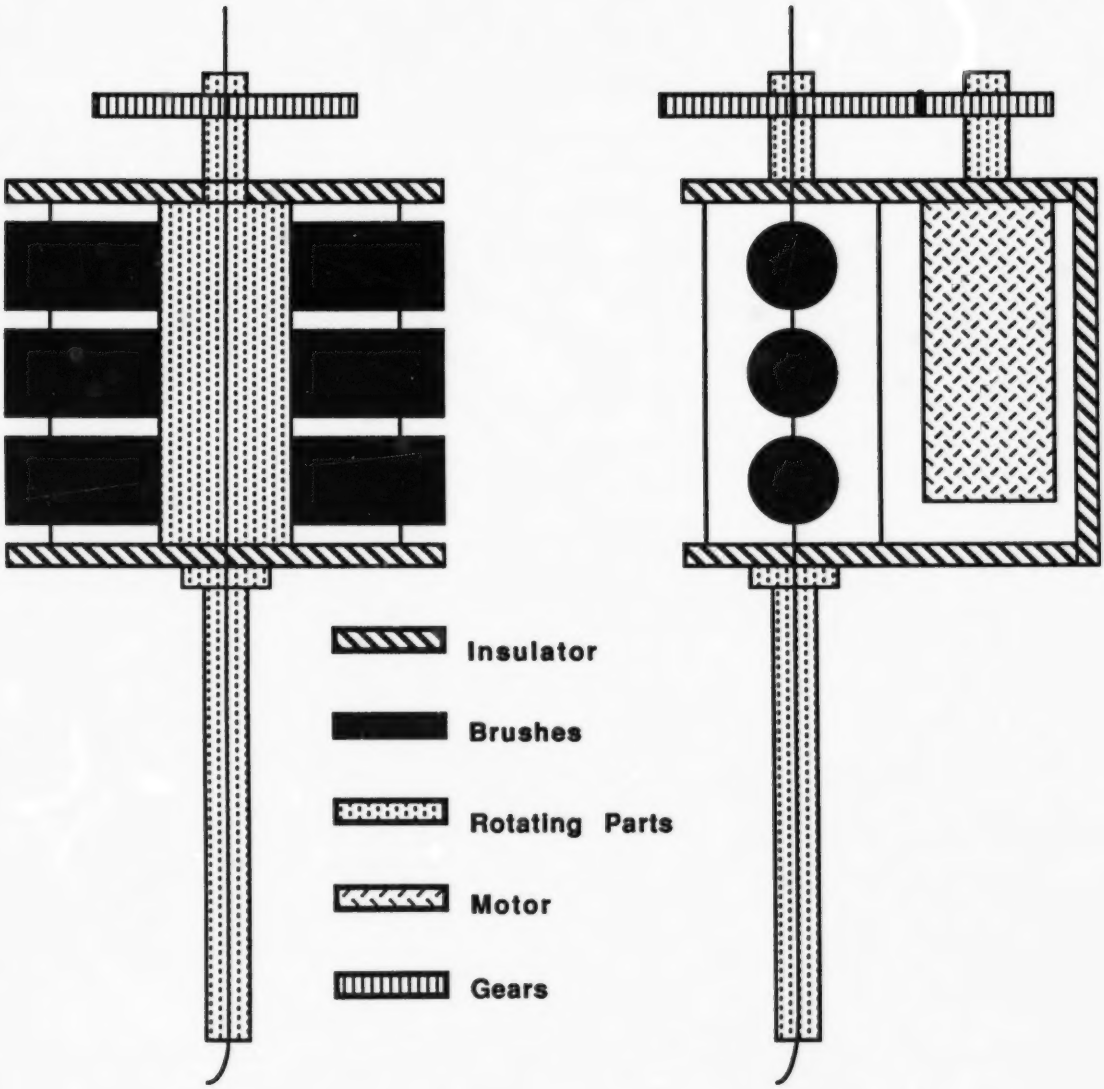

Figure C1. Experimental Rotating Arc Torch